

The magnetic phase diagram of $\text{Gd}_2\text{Sn}_2\text{O}_7$

This article has been downloaded from IOPscience. Please scroll down to see the full text article.

2011 J. Phys.: Condens. Matter 23 164215

(<http://iopscience.iop.org/0953-8984/23/16/164215>)

View [the table of contents for this issue](#), or go to the [journal homepage](#) for more

Download details:

IP Address: 71.179.252.34

The article was downloaded on 22/05/2011 at 02:35

Please note that [terms and conditions apply](#).

The magnetic phase diagram of $\text{Gd}_2\text{Sn}_2\text{O}_7$

R S Freitas¹ and J S Gardner^{2,3}

¹ Instituto de Física, Universidade de São Paulo, CP 66318, 05314-970 São Paulo, SP, Brazil

² Indiana University, Bloomington, IN 47408, USA

³ NCNR, NIST, Gaithersburg, MD 20899-6102, USA

E-mail: freitas@if.usp.br

Received 6 November 2010, in final form 25 February 2011

Published 6 April 2011

Online at stacks.iop.org/JPhysCM/23/164215

Abstract

Measurements of the magnetic susceptibility of the frustrated pyrochlore magnet $\text{Gd}_2\text{Sn}_2\text{O}_7$ have been performed at temperatures below $T = 5$ K and in magnetic fields up to $H = 12$ T. The phase boundaries determined from these measurements are mapped out in an H - T phase diagram. In this gadolinium compound, where the crystal-field splitting is small and the exchange and dipolar energy are comparable, the Zeeman energy overcomes these competing energies, resulting in at least four magnetic phase transitions below 1 K. These data are compared against those for $\text{Gd}_2\text{Ti}_2\text{O}_7$ and will, we hope, stimulate further studies.

(Some figures in this article are in colour only in the electronic version)

1. Introduction

The strong correlation between lattice, electronic, and magnetic degrees of freedom in several materials has been the subject of intense research in recent years [1]. This mutual coupling results in a delicate balance between the different possible ground states and can play a crucial role defining the macroscopic properties of a material. Geometrically frustrated magnetic systems are a prime example of the rich behavior that can result from such strong correlations [2, 3]. In these systems the geometry of the lattice prevents the simultaneous minimization of all pairwise magnetic interactions, which are called frustrated, resulting in a myriad of different and unusual ground states. These include, among others, the spin ice state in $\text{Ho}_2\text{Ti}_2\text{O}_7$ and $\text{Dy}_2\text{Ti}_2\text{O}_7$ [4], the spin liquid behavior in $\text{Tb}_2\text{Ti}_2\text{O}_7$ [5] and the spin glass state with minimum disorder in $\text{Y}_2\text{Mo}_2\text{O}_7$ [6]. All these systems share the same crystallographic structure composed of corner-sharing tetrahedra, the so-called pyrochlore lattice [7]. These materials often show strong sensibility to small external perturbations such as, for example, the applied magnetic field, which can induce interesting collective behavior [8, 9].

The gadolinium compounds, $\text{Gd}_2\text{Ti}_2\text{O}_7$ and $\text{Gd}_2\text{Sn}_2\text{O}_7$, are expected to have very small intrinsic anisotropy since the Gd^{3+} ions are in a state with $S = 7/2$ and $L = 0$. However, the Gd^{3+} ions occupy a site with trigonal symmetry and spin-orbit coupling, arising from mixing of the energy levels with $L \neq 0$, will result in the addition of a small amount of anisotropy to their character. Additionally, Curie-Weiss analysis of

the dc magnetic susceptibility indicates antiferromagnetic interactions between the Gd spins in both compounds with a Curie-Weiss temperature $\theta_{\text{CW}} \sim -9$ K [10–12]. Therefore, they were expected to be a good realization of a Heisenberg antiferromagnet on a pyrochlore lattice which, according to theoretical calculations that include nearest-neighbor exchange only, should possess a disordered ground state [13]. When dipole-dipole coupling is included [10, 14] the system has a tendency to order. Experimentally, both compounds exhibit phase transitions to ordered ground states. In $\text{Gd}_2\text{Ti}_2\text{O}_7$ two magnetic transitions at $T_1 \sim 1$ K and $T_2 \sim 0.7$ K have been observed [11], and in $\text{Gd}_2\text{Sn}_2\text{O}_7$ one transition has been detected at $T_N \sim 1$ K [12]. Despite the similarity of the lattice parameter of both Ti and Sn compounds the nature of the observed ground state is quite different. Neutron diffraction studies for $\text{Gd}_2\text{Ti}_2\text{O}_7$ [15–17] revealed an ordered structure. Stewart *et al* [16] found that between T_1 and T_2 , 3/4 of the spins are frozen along local $\langle 110 \rangle$ directions, whilst the full moment and the others are paramagnetic. This 4- \mathbf{k} structure remains below T_2 but the disordered sublattice acquires a small ordered moment. In $\text{Gd}_2\text{Sn}_2\text{O}_7$, neutron diffraction by Wills *et al* [18] confirmed the presence of the four-sublattice Néel state with $\mathbf{k} = (000)$, an antiferromagnetic arrangement predicted by Palmer and Chalker using mean field calculations including quartic terms in the free energy [14].

The influence of a magnetic field has been studied for $\text{Gd}_2\text{Ti}_2\text{O}_7$. A polycrystalline study by Ramirez *et al* [11] and more recently a single crystal study by Petrenko *et al* [19] found four different field-driven phases. The single

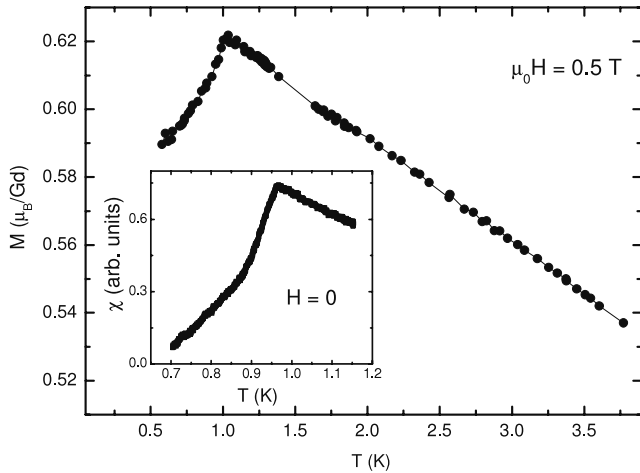


Figure 1. Temperature dependence of the magnetization of $\text{Gd}_2\text{Sn}_2\text{O}_7$ measured in an applied field of $\mu_0 H = 0.5$ T. The inset shows the ac susceptibility as a function of temperature measured with modulation field $\mu_0 h_{ac} = 1$ mT and $\mu_0 H = 0$ T. Due to temperature stability problems, data collected around 1.5 K was removed from the magnetization data.

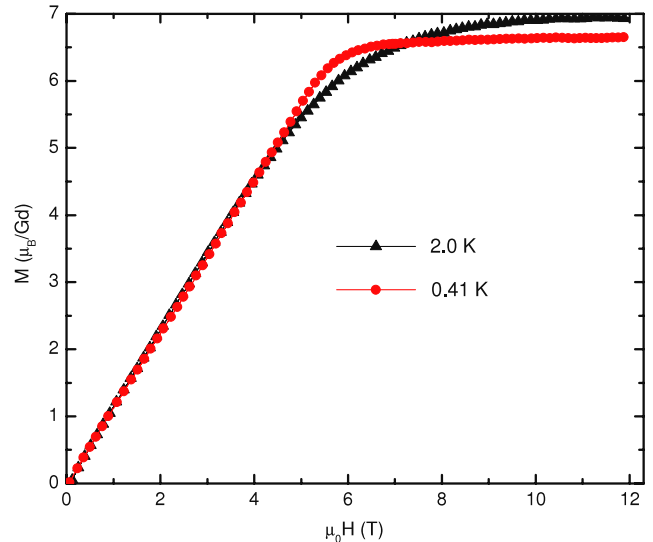


Figure 2. Magnetization as a function of field of $\text{Gd}_2\text{Sn}_2\text{O}_7$ at $T = 2$ and 0.41 K up to applied fields of $\mu_0 H = 12$ T.

crystal work found that when the field is applied along a given crystallographic direction only three phases exist [19] and by considering fields along the [110], [111] and [112] they reproduced the polycrystalline phase diagram. The existence of a complex phase diagram in a system with negligible anisotropy is very unusual, but Glazkov *et al* [20] have recently found evidence of a single-ion anisotropy with strength comparable with the strength of the exchange coupling for both Ti and Sn compounds. Their electron spin resonance experiments found the main anisotropy constant, D , is equal to 0.223 K and 0.140 K for $\text{Gd}_2\text{Ti}_2\text{O}_7$ and $\text{Gd}_2\text{Sn}_2\text{O}_7$, respectively. These are approximately 60% of the respective exchange coupling, J , for each compound. A more recent polycrystalline neutron scattering study on $\text{Gd}_2\text{Sn}_2\text{O}_7$ [21] confirmed the existence of the Palmer–Chalker ground state and a gapped excitation spectrum in zero field, predicted earlier by Del Maestro and Gingras [22] and it is therefore believed that we have a good understanding of this pyrochlore, at least in zero field. Stewart *et al* [21] went on to apply a magnetic field to their polycrystalline sample and observed multiple changes to the ratio of Bragg peak intensities, indicative of multiple magnetic phase transitions. Here we have used ac susceptibility to elucidate these magnetic transitions and to determine the $\mu_0 H(T)$ phase diagram of $\text{Gd}_2\text{Sn}_2\text{O}_7$.

2. Experimental details

A polycrystalline sample of $\text{Gd}_2\text{Sn}_2\text{O}_7$ was prepared by high-temperature solid-state reaction. The powder x-ray diffraction confirmed that the sample was single phase. Magnetization was measured using a vibration sample magnetometer (VSM) and ac susceptibility was measured using a mutual inductance bridge operating at modulation frequency $f = 155$ Hz and ac field $\mu_0 h_{ac} = 1$ mT. Both measurements were made in a ^3He refrigerator system in the presence of magnetic fields up to 12 T.

3. Results and discussion

Figure 1 shows the temperature dependence of the dc magnetization and ac susceptibility (inset) of $\text{Gd}_2\text{Sn}_2\text{O}_7$. Both measurements display a cusp like anomaly close to 1 K in agreement with previous magnetic [12] and calorimetric [23] studies. This anomaly is identified as the transition, $T_N \sim 1$ K, to the antiferromagnetic ground state. These measurements are consistent with those published elsewhere and result in a frustration index, $\theta_{CW}/T_N \sim 10$. Isothermal magnetization curves were measured above and below T_N and are presented in figure 2. At 2 K, just above the transition temperature T_N , the sample reaches a saturation moment of $6.95(5) \mu_B/\text{Gd}$ in excellent agreement with the theoretical expected value $g\mu_B S = 7 \mu_B$ and consistent with Sosin *et al* [24] who observed a fully saturated moment above 8 T at 1.75 K. Below the transition temperature at 0.41 K the magnetization is linear in field over a wide range up to $\mu_0 H = 5.3$ T, followed by a plateau with a moment of $6.65(5) \mu_B/\text{Gd}$, which is somewhat lower than the theoretical saturation value but easily measured within the present experimental accuracy. Although small, the difference between the plateau and the saturation value may indicate that below T_N the system is in a metastable, unsaturated, phase with part of the spins pinned by the local interaction and pointing in a different direction from the applied magnetic field. It should be mentioned here that at 0.3 K in 55 T, $\text{Gd}_2\text{Ti}_2\text{O}_7$ does not reach a fully saturated state of $7 \mu_B$, but instead a plateau is seen above 6 T at $6.8(1) \mu_B/\text{Gd}$ [25] and at 1.3 K, the moment appears not to saturate in 55 T.

We present in figure 3 the field dependence of the ac susceptibility χ measured at different temperatures. As the field is increased the susceptibility displays a sharp downturn and extrapolates to zero for field values around 8 T. This is consistent with the saturation of the magnetization observed at the same field range and low temperatures in figure 2.

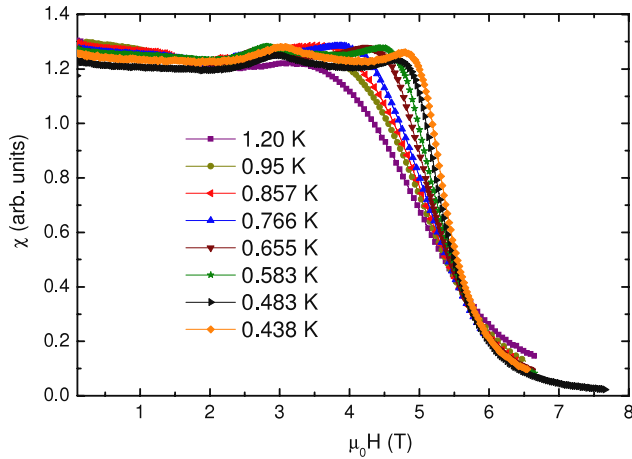


Figure 3. Field dependence of ac susceptibility for $Gd_2Sn_2O_7$ at selected temperatures.

Also clear in the figure is the temperature dependence of the initial downturn in the susceptibility with increasing magnetic field, and a small temperature dependent hump visible for fields close below 3 T. The high sensitivity of the ac susceptibility technique allows the identification of several field-induced phase transitions as anomalies in its field $\chi(H)$ and temperature $\chi(T)$ dependence. In figure 4(a) we show an enlargement of the low-field region of $\chi(H)$ isotherms measured at different temperatures. The curve measured at 0.857 K exhibit a kink at 1.4 T and two peaks centered at 2.2 and 3.5 T. With the decrease in the measuring temperature the low-field kink becomes smeared while the two high-field peaks get increasingly well defined. Figure 4(b) display $\chi(T)$ measured with $\mu_0H = 1.0, 1.25$ and 1.5 T. As the temperature is lowered the susceptibility shows a broad feature followed by a sharp peak, which moves to lower temperatures with the increase of the measuring magnetic field. The emergence of the broad feature is probably associated with short-range order and can be correlated with the broad, diffuse magnetic scattering seen in the neutron experiments by Stewart *et al* [21].

The magnetic phase diagram for $Gd_2Sn_2O_7$ obtained by plotting the field dependence of the temperature anomalies observed in the magnetic susceptibility is shown in figure 5.

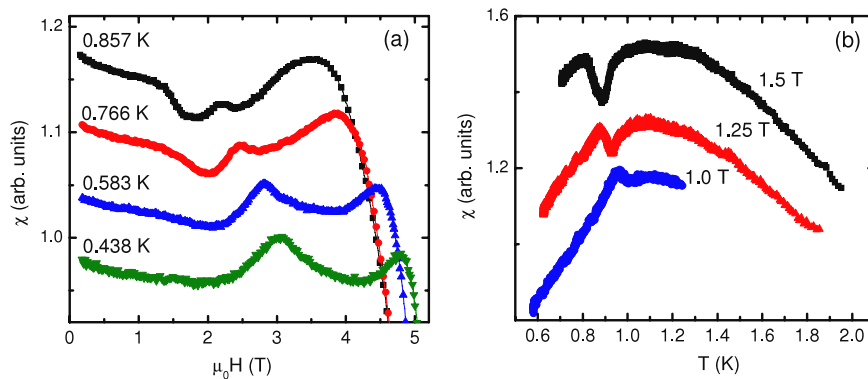


Figure 4. (a) Field dependence of ac susceptibility measured at different temperatures. (b) The temperature dependence of ac susceptibility measured with 1.5, 1.25 and 1.0 T for $Gd_2Sn_2O_7$.

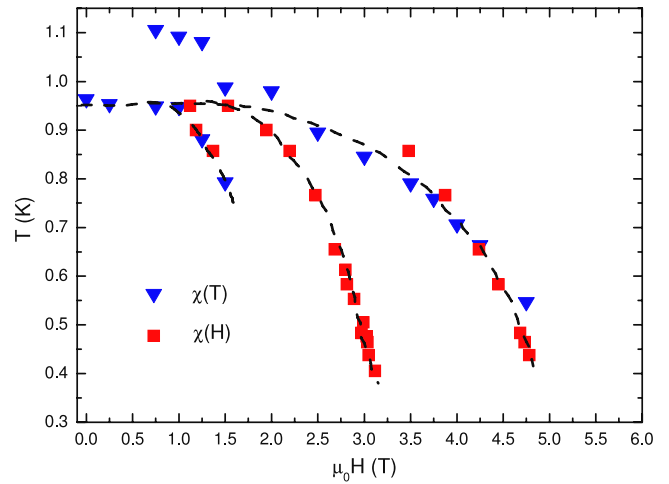


Figure 5. Phase diagram of $Gd_2Sn_2O_7$. Triangles and squares denote the positions of anomalies in the ac susceptibility measured as a function of temperature and magnetic field, respectively. The lines are guides to the eyes.

The data points at high temperatures correspond to the center of the broad transitions observed in $\chi(T)$ and as explained above are associated with short range spatially correlated spins. Below ~ 0.95 K three different magnetic phases can be distinguished with the increase in the magnetic field. In zero and low fields ($\mu_0H < 1$ T) only one transition is seen at approximately 1 K, consistent with results previously published [12, 23, 26, 27].

A kink in $\chi(H)$ and the sharp peak in $\chi(T)$ that elucidates the lowest field dependent phase boundary could not be followed below 0.8 K, possibly due to the fact that the kink in $\chi(H)$ is obscured by the intense peak that defines the intermediate field phase boundary. Nevertheless, the extrapolation of this transition line to lower temperatures is consistent with the phase boundary found close to 2.5 T by Stewart *et al* [21]. The intermediate and the high-field transition lines of figure 5 extrapolate to approximately 3.5 and 5.5 T at 50 mK. We note that around these field values considerable intensity changes in different Bragg peaks are also observed in [21] and 5.8 T is the calculated saturation field from electron spin resonance measurements [28].

In summary, we have determined the phase diagram of polycrystalline $\text{Gd}_2\text{Sn}_2\text{O}_7$. This geometrically frustrated magnet is well described by the Palmer–Chalker model [14] and the measured zero-field properties [21, 23] have been reproduced from linear spin wave calculations [22] starting from this ground state. When an external field is applied to the ordered ground state several new magnetic phases are observed before the system is completely polarized around 6 T. This complex phase diagram is reminiscent of that in the other dipolar Heisenberg magnet $\text{Gd}_2\text{Ti}_2\text{O}_7$ [11], however the zero-field state is not hindered by the complicated phase separation [17]. We believe this study will stimulate others to perform more measurements, specifically single crystal neutron scattering and susceptibility studies, and theorists calculating these properties in an external magnetic field.

Acknowledgments

RSF acknowledges support from FAPESP (08/00457-2) and CNPq-Brazil (471188/2008-5). JSG acknowledges support from the National Science Foundation under Agreement No. DMR-0944772.

References

- [1] Dagotto E 2002 *Nanoscale Phase Separation and Colossal Magnetoresistance* (Berlin: Springer)
- [2] Ramirez A P 1994 *Annu. Rev. Mater. Sci.* **24** 453
- [3] Urano C, Nohara M, Kondo S, Sakai F, Takagi H, Shiraki T and Okubo T 2000 *Phys. Rev. Lett.* **85** 1052
- [4] Ramirez A P, Hayashi A, Cava R J, Siddharthan R and Shastry B S 1999 *Nature* **399** 333
Bramwell S T and Gingras M J P *Science* **294** 1495
- [5] Gardner J S *et al* 1999 *Phys. Rev. Lett.* **82** 1012
Kao Y-J, Enjalran M, Del Maestro A G, Molavian H R and Gingras M J P 2003 *Phys. Rev. B* **68** 172407
Molavian H R, Gingras M J P and Canals B 2007 *Phys. Rev. Lett* **98** 157204
- [6] Greedan J E, Sato M, Yan X U and Razavi F S 1986 *Solid State Commun.* **59** 895
Gingras M J P, Stager C V, Raju N P, Gaulin B D and Greedan J E 1997 *Phys. Rev. Lett.* **78** 947
Gardner J S, Gaulin B D, Lee S H, Broholm C, Raju N P and Greedan J E 1999 *Phys. Rev. Lett.* **83** 211
- [7] Gardner J S, Gingras M J P and Greedan J E 2010 *Rev. Mod. Phys.* **82** 53
- [8] Higashinaka R and Maeno Y 2005 *Phys. Rev. Lett.* **95** 237208
- [9] Fennell T, Bramwell S T, McMorrow D F, Manuel P and Wildes A R 2007 *Nature Phys.* **8** 566
- [10] Raju N P, Dion M, Gingras M J P, Mason T E and Greedan J E 1999 *Phys. Rev. B* **59** 14489
- [11] Ramirez A P, Shastry B S, Hayashi A, Krajewski J J, Huse D A and Cava R J 2002 *Phys. Rev. Lett.* **89** 067202
- [12] Bonville P, Hodges J A, Ocio M, Sanchez J P, Vulliet P, Sosin S and Braithwaite D 2003 *J. Phys.: Condens. Matter* **15** 7777
- [13] Reimers J N, Berlinsky A J and Shi A C 1991 *Phys. Rev. B* **43** 865
Moessner R and Chalker J T 1998 *Phys. Rev. Lett.* **80** 2929
Moessner R and Chalker J T 1998 *Phys. Rev. B* **58** 12049
- [14] Palmer S E and Chalker J T 2000 *Phys. Rev. B* **62** 488
- [15] Champion J D M, Wills A S, Fennell T, Bramwell S T, Gardner J S and Green M A 2001 *Phys. Rev. B* **64** 140407
- [16] Stewart J R, Ehlers G, Wills A S, Bramwell S T and Gardner J S 2004 *J. Phys.: Condens. Matter* **16** L321
- [17] Gardner J S, Stewart J R and Ehlers G 2009 *AIP Conf. Proc.* **1202** 3
- [18] Wills A S, Zhitomirsky M E, Canals B, Sanchez J P, Bonville P, Dalmas de Réotier P and Yaouanc A 2006 *J. Phys.: Condens. Matter* **18** L37
- [19] Petrenko O A, Lees M R, Balakrishnan G and Paul D M 2004 *Phys. Rev. B* **70** 012402
- [20] Glazkov V N *et al* 2007 *J. Phys.: Condens. Matter* **19** 145271
- [21] Stewart J R, Gardner J S, Qiu Y and Ehlers G 2008 *Phys. Rev. B* **78** 132410
- [22] Del Maestro A G and Gingras M J P 2007 *Phys. Rev. B* **76** 064418
- [23] Quilliam J A, Ross K A, Del Maestro A G, Gingras M J P, Corruccini L R and Kycia J B 2007 *Phys. Rev. Lett.* **99** 097201
- [24] Sosin S S, Prozorova L A, Smirnov A I, Bonville P, Jasmin-Le Bras G and Petrenko O 2008 *Phys. Rev. B* **77** 104424
- [25] Narumi Y, Kikkawa A, Katsumata K, Honda Z, Hagiwara M and Kindo K 2006 *AIP Conf. Proc.* **850** 1113
- [26] Luo G, Hess S T and Corruccini L R 2001 *Phys. Lett. A* **291** 306
- [27] Chapuis Y, Dalmas de Réotier P, Marin C, Yaouanc A, Forget A, Amato A and Baines C 2009 *Physica B* **404** 686
- [28] Sosin S S, Prozorova L A, Bonville P and Zhitomirsky M E 2009 *Phys. Rev. B* **79** 014419